

# Spherical autoregressive change-point detection with applications

## *Stima del punto di cambio mediante modelli autoregressivi sulla sfera e sue applicazioni*

Federica Spoto, Alessia Caponera and Pierpaolo Brutti

**Abstract** Spatio-temporal processes arise very naturally in a number of different applied fields, like Cosmology, Astrophysics, Geophysics, Climate and Atmospheric Science. In most of these areas, the detection of structural breaks or regime shifts in the data stream is key. To this end, in the present work, we aim at generalizing the recently introduced SPHAR(p) process by allowing for temporal changes in its functional parameters and variability structure. Our approach, which intrinsically integrates the spatial and temporal dimensions, could give multiscale insights into both the global and local behavior of changes, and its performance will be tested on a real dataset of global surface temperature anomalies.

**Abstract** *I processi spatio-temporali sorgono naturalmente in numerosi campi applicativi, come la Cosmologia, l'Astrofisica, la Geofisica, le Scienze del Clima e dell'Atmosfera. In molti di questi ambiti, l'individuazione di break strutturali nella serie dei dati è fondamentale. A tal fine, nel presente lavoro, ci proponiamo di generalizzare i processi SPHAR(p) introducendo cambiamenti temporali nei parametri funzionali e nella loro struttura di variabilità. Il nostro approccio, oltre ad integrare esplicitamente sia la dimensione spaziale che quella temporale del fenomeno in studio, permette al contempo di estrarre informazioni multiscala che meglio qualificano e caratterizzano i punti di cambio individuati. Le prestazioni della modellistica proposta saranno testate su un dataset reale relativo ad anomalie della temperatura superficiale globale.*

**Key words:** Spherical Functional Autoregressions, Change-point model, Spatio-temporal model, Global climate change

---

Federica Spoto  
Sapienza University of Rome, e-mail: federica.spoto@uniroma1.it

Alessia Caponera  
École Polytechnique Fédérale de Lausanne, e-mail: alessia.caponera@epfl.ch

Pierpaolo Brutti  
Sapienza University of Rome, e-mail: pierpaolo.brutti@uniroma1.it

## 1 Introduction

Over the last few decades, the study of random fields on the sphere has received increasing attention because of their real-life applications in a variety of different areas like Cosmology, Astrophysics, Climatology and many more. In most of these areas, the detection of structural breaks or regime shifts in the data stream is key. In Climate Sciences, for example, variations in the rate at which global surface temperatures evolve is the most prominent and widely studied footprint of global warming. Despite this, the vast majority of such analyses are purely temporal or do not take into account the spatial dependence. A few notable exceptions are [2], [1] and [9].

In the present work, we aim at generalizing the recently introduced SPHAR( $p$ ) process by allowing for temporal changes in its functional parameters and variability structure. Our approach, which intrinsically integrates the spatial and temporal dimensions, could give multiscale insights into both the global and local behavior of changes.

## 2 Materials and Methods

### 2.1 Spherical functional autoregressions

Working in a functional time series setup, we focus on time-varying spherical random field  $\{T(x, t) : (x, t) \in \mathbb{S}^2 \times \mathbb{Z}\}$  which exhibits a discrete temporal dynamics over the unit sphere  $\mathbb{S}^2$  so that, for every fixed  $t \in \mathbb{Z}$ , the field  $T_t \equiv T(\cdot, t)$  is a random element of  $L^2(\mathbb{S}^2)$  (the space of square-integrable functions on the unit sphere), and admits a characterization in terms of spherical functional autoregressive models as described in [6, 7].

Specifically, sphere-cross-time random fields belonging to the class of spherical functional autoregressions of order  $p$  (SPHAR( $p$ )) satisfy

$$T(x, t) = \sum_{i=1}^p (\Phi_i T_{t-i})(x) + Z(x, t), \quad \forall (x, t) \in \mathbb{S}^2 \times \mathbb{Z}, \quad (1)$$

where  $\{Z(x, t) : (x, t) \in \mathbb{S}^2 \times \mathbb{Z}\}$  is a Gaussian isotropic spherical white noise and  $\{\Phi_i : i = 1, \dots, p\}$  are integral operators on  $L^2(\mathbb{S}^2)$  associated with  $p$  continuous isotropic kernels  $\{k_i : i = 1, \dots, p\}$ ; see [7] for more formal and detailed definitions. Such processes can be interpreted as a generalization of autoregressive (AR( $p$ )) processes, taking values on  $L^2(\mathbb{S}^2)$ , rather than on the real line (see also [3]).

The existence of a unique spatially isotropic and temporally stationary solution for Equation (1) is guaranteed by assuming some conditions on the  $\Phi_i$ 's. For instance, when  $p = 1$ , a necessary and sufficient condition is given by  $\|\Phi\|_{\text{op}} =$

$\max_{\ell \in \mathbb{N}} |\phi_\ell| < 1$ , where the  $\phi_\ell$ 's are the eigenvalues of  $\Phi$ . See [5] for an in-depth discussion.

It is well known that the following spectral representation holds in  $L^2(\Omega)$

$$T(x, t) = \sum_{\ell=0}^{\infty} \sum_{m=-\ell}^{\ell} a_{\ell,m}(t) Y_{\ell,m}(x), \quad \forall (x, t) \in \mathbb{S}^2 \times \mathbb{Z},$$

where the set  $\{Y_{\ell,m}(\cdot) : \ell \geq 0, m = -\ell, \dots, \ell\}$  is a standard basis for  $L^2(\mathbb{S}^2)$  of real-valued spherical harmonics (see, e.g., [11]), and  $\{a_{\ell,m}(\cdot) : \ell \geq 0, m = -\ell, \dots, \ell\}$  are the (random) generalized Fourier coefficients defined as  $a_{\ell,m}(t) = \langle T_t, Y_{\ell,m} \rangle_{L^2}$  and satisfying

$$\mathbb{E}[a_{\ell,m}(t) a_{\ell',m'}(s)] = 0, \quad \text{for } \ell \neq \ell', m \neq m'.$$

Moreover, for every fixed  $(\ell, m)$ , it is possible to show that

$$a_{\ell,m}(t) = \sum_{i=1}^p \phi_{\ell,i} a_{\ell,m}(t-i) + \varepsilon_{\ell,m}(t), \quad \forall t \in \mathbb{Z},$$

where  $\{\varepsilon_{\ell,m}(t) = \langle Z_t, Y_{\ell,m} \rangle_{L^2} : t \in \mathbb{Z}\}$  is a Gaussian white noise with variance  $\sigma_\ell^2 > 0$ . Note that the  $\phi_{\ell,i}$ 's and  $\sigma_\ell^2$  do not depend on  $m$ , as a consequence of isotropy.

## 2.2 Spherical change-point detection

Under the assumptions described in the previous section, we introduce the spherical autoregressive change-point model and the methodology to detect possible change-points in the data. For the sake of simplicity, our arguments are presented for a SPHAR(1) model, allowing a single change-point; however, the analysis can be generalized to higher autoregressive orders and multiple change-points. In this setting, the model is written as the composition of two stationary SPHAR segments and takes the form

$$T(x, t) = \begin{cases} (\Phi_1 T_{t-1})(x) + Z_1(x, t) & t < \tau \\ (\Phi_2 T_{t-1})(x) + Z_2(x, t) & t \geq \tau \end{cases},$$

that, given  $\tau$ , are assumed to be independent; equivalently, thanks to the spectral representation, one can jointly look at

$$a_{\ell,m}(t) = \begin{cases} \phi_{\ell;1} a_{\ell,m}(t-1) + \varepsilon_{\ell,m;1}(t) & t < \tau \\ \phi_{\ell;2} a_{\ell,m}(t-1) + \varepsilon_{\ell,m;2}(t) & t \geq \tau \end{cases}, \quad \ell \geq 0, m = -\ell, \dots, \ell.$$

The task consists in detecting the time-stamp  $\tau$  at which the model parameters have a variation in value. The optimal change-point is selected through a model choice criteria based on information theory.

Throughout this paper, we shall assume to be able to observe a finite set of Fourier coefficients

$$\alpha = \{a_{\ell,m}(t) : t = 1, \dots, n, \ell = 0, \dots, L, m = -\ell, \dots, \ell\}.$$

Given  $\tau$  and for fixed  $(\ell, m)$ , one can define the vectors

$$\alpha_{\ell,m;1} = (a_{\ell,m}(1), \dots, a_{\ell,m}(\tau - 1))^T, \quad \alpha_{\ell,m;2} = (a_{\ell,m}(\tau), \dots, a_{\ell,m}(n))^T,$$

of dimensions  $n_1$  and  $n_2$ , respectively. Thus, for  $j = 1, 2$ ,

$$\mathbb{E}[\alpha_{\ell,m;j} \alpha_{\ell,m;j}^T] = \sigma_{\ell,j}^2 V_{\ell;j},$$

where  $\sigma_{\ell,j}^2$  is the noise variance and  $V_{\ell;j}$  is a  $n_j \times n_j$  symmetric and positive definite matrix depending on  $\phi_{\ell,j}$ . The likelihood function for the parameters  $\theta = \{\phi_{\ell,j}, \sigma_{\ell,j}^2, \ell = 0, \dots, L, j = 1, 2\}$  and  $\tau$  is then

$$L(\theta, \tau; \alpha) = \prod_{\ell=0}^L \prod_{m=-\ell}^{\ell} \prod_{j=1}^2 (2\pi\sigma_{\ell,j}^2)^{-n_j/2} |V_{\ell;j}|^{-1/2} \exp \left\{ -\frac{1}{2\sigma_{\ell,j}^2} \alpha_{\ell,m;j}^T V_{\ell;j}^{-1} \alpha_{\ell,m;j} \right\};$$

moreover, using the standard approximation to the log-likelihood for AR models (see [4]), one gets

$$-\frac{2}{n} \log L(\hat{\theta}, \tau; \alpha) = \frac{1}{n} \sum_{\ell=0}^L (2\ell + 1) \sum_{j=1}^2 n_j \log(2\pi\hat{\sigma}_{\ell,j}^2) + (L + 1)^2 + o_L(1),$$

with  $\hat{\theta} = (\hat{\phi}_{\ell,j}, \hat{\sigma}_{\ell,j}^2, \ell = 0, \dots, L, j = 1, 2)^T$  being the corresponding maximum likelihood estimate (MLE) of  $\theta$ . Hence,  $\hat{\tau}$  can be defined as the value that minimizes

$$R(\tau) = \sum_{\ell=0}^L (2\ell + 1) \sum_{j=1}^2 n_j \log(2\pi\hat{\sigma}_{\ell,j}^2). \tag{2}$$

Note that this is equivalent to minimize the AIC score, since the number of parameters is constant. In addition, for computational reasons, one may replace the MLE estimate of  $\sigma_{\ell,j}^2$  with the Yule-Walker or least squares estimates, due to their equivalence in large sample size regimes.

### 3 Results

The methodology presented above was applied to *global (land and ocean) surface temperature anomalies*. More in detail, the dataset is built starting from the NCEP/NCAR monthly averages of the surface air temperature (in degrees Celsius) from 1948 to 2020, over a global grid with 2.5° spacing for latitude and longi-

tude, see [10]. Following the World Meteorological Organization policy, temperature anomalies are obtained by subtracting the long-term monthly means relative to the 1981–2010 base period. They are then averaged over months to switch from a monthly scale to an annual scale.

By means of the `healpix` package (see [8] and the official `healpix` website), we converted the gridded data into spherical maps with a resolution of  $12 \cdot \text{NSIDE}^2$  pixels ( $\text{NSIDE} = 16$ ) and then we computed the Fourier coefficients up to  $L = 2 \cdot \text{NSIDE}$ .

In order to handle possible anisotropies in the mean, for each segment  $j = 1, 2$ , we introduced an intercept  $\mu_j \in L^2(\mathbb{S}^2)$ , which has a representation in terms of spherical harmonics

$$\mu_j = \sum_{\ell=0}^{\infty} \sum_{m=-\ell}^{\ell} \mu_{\ell,m;j} Y_{\ell,m}, \quad \text{in } L^2(\mathbb{S}^2),$$

with  $\mu_{\ell,m;j} = \langle \mu_j, Y_{\ell,m} \rangle_{L^2}$ .

By minimizing (2) over  $\tau \in \{1953, \dots, 2016\}$ , the best change point results to be  $\hat{\tau} = 1982$ . Then, we can estimate the functional parameters  $(\mu_j, \Phi_j)$  by solving the following least-squares minimization problem, see [6, 7],

$$(\hat{\mu}_j, \hat{\Phi}_j) := \operatorname{argmin} \sum_{t \in \mathcal{T}_j} \|T_t - \mu_{j:L} - \Phi_{j:L} T_{t-1}\|_{L^2(\mathbb{S}^2)}^2,$$

where  $\mu_{j:L}$  and  $\Phi_{j:L}$  are the truncated version of  $\mu_j$  and  $\Phi_j$ , respectively, and  $\mathcal{T}_j$  is the set of time-stamps belonging to each segment, i.e.  $\mathcal{T}_1 = \{1949, \dots, \hat{\tau} - 1\}$  and  $\mathcal{T}_2 = \{\hat{\tau}, \dots, 2020\}$ .

The comparison between the two periods can be carried out by computing the two mean surfaces

$$(I_L - \hat{\Phi}_j)^{-1} \hat{\mu}_j = \sum_{\ell=0}^L \sum_{m=-\ell}^{\ell} \frac{\hat{\mu}_{\ell,m;j}}{1 - \hat{\Phi}_{\ell;j}} Y_{\ell,m}, \quad j = 1, 2.$$

Figure 1 shows the estimated mean surfaces pre and post  $\hat{\tau} = 1982$  (on the same color scale) and their difference. A positive anomaly indicates that the observed temperature was warmer than the reference value, while a negative anomaly indicates that the observed temperature was cooler than the reference value.

The analysis suggests an overall increase in the mean surface temperature anomalies, which is particularly evident for the North and South poles.

## References

1. Altieri, L., Cocchi, D., Greco, F., Illian, J., Scott, E.: Bayesian P-splines and advanced computing in R for a changepoint analysis on spatio-temporal point processes. *Journal of Statistical Computation and Simulation* **86**(13), 2531–2545 (2016)

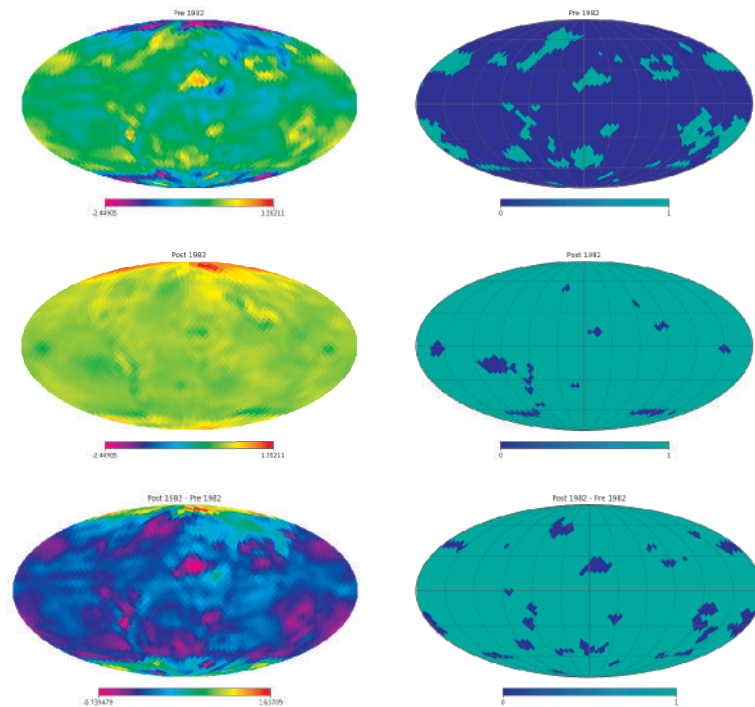


Fig. 1: Left: estimated mean surfaces pre and post  $\hat{\tau} = 1982$  (on the same color scale) and their difference. Right: corresponding negative (0) and positive (1) pixels.

2. Altieri, L., Scott, E.M., Cocchi, D., Illian, J.B.: A changepoint analysis of spatio-temporal point processes. *Spatial Statistics* **14**, 197–207 (2015). Spatio-Temporal Stochastic Modelling of Environmental Hazards
3. Bosq, D.: *Linear Processes in Function Spaces: Theory and Applications*. Springer (2000)
4. Brockwell, P., Davis, R.: *Time Series: Theory and Methods: Theory and Methods*. Springer Series in Statistics. Springer New York (1991)
5. Caponera, A.: SPHARMA approximations for stationary functional time series on the sphere (2020). arXiv:2009.13189
6. Caponera, A.: Statistical inference for spherical functional autoregressions. PhD Thesis, Sapienza University of Rome (2020)
7. Caponera, A., Marinucci, D.: Asymptotics for spherical functional autoregressions. *Annals of Statistics* **49**(1), 346–369 (2021)
8. Gorski, K.M., Hivon, E., Banday, A.J., Wandelt, B.D., Hansen, F.K., Reinecke, M., Bartelmann, M.: HEALPix: A framework for high-resolution discretization and fast analysis of data distributed on the sphere. *The Astrophysical Journal* **622**(2), 759–771 (2005)
9. Jun, M.: Matérn-based nonstationary cross-covariance models for global processes. *Journal of Multivariate Analysis* **128**, 134–146 (2014)
10. Kalnay, E., et al.: The NCEP/NCAR 40-year reanalysis project. *Bulletin of the American Meteorological Society* **77**(3), 437–472 (1996)
11. Marinucci, D., Peccati, G.: *Random Fields on the Sphere: Representation, Limit Theorems and Cosmological Applications*. London Mathematical Society Lecture Note Series. Cambridge University Press (2011)